

Durham Research Online

Deposited in DRO:

06 November 2018

Version of attached file:

Accepted Version

Peer-review status of attached file:

Peer-reviewed

Citation for published item:

Colella, Marco and Pander, Piotr Henryk and Pereira, Daniel De Sa and Monkman, Andrew P. (2018) 'Interfacial TADF exciplex as a tool to localise excitons, improve efficiency and increase OLED lifetime.', *ACS applied materials interfaces.*, 10 (46). pp. 40001-40007.

Further information on publisher's website:

<https://doi.org/10.1021/acsami.8b15942>

Publisher's copyright statement:

This document is the Accepted Manuscript version of a Published Work that appeared in final form in *ACS applied materials interfaces* copyright © American Chemical Society after peer review and technical editing by the publisher. To access the final edited and published work see <https://doi.org/10.1021/acsami.8b15942>

Additional information:

Use policy

The full-text may be used and/or reproduced, and given to third parties in any format or medium, without prior permission or charge, for personal research or study, educational, or not-for-profit purposes provided that:

- a full bibliographic reference is made to the original source
- a [link](#) is made to the metadata record in DRO
- the full-text is not changed in any way

The full-text must not be sold in any format or medium without the formal permission of the copyright holders.

Please consult the [full DRO policy](#) for further details.

**Interfacial TADF Exciplex as a Tool to Localise Excitons,
Improve Efficiency and Increase OLED Lifetime**

Marco Colella, Piotr Henryk Pander, Daniel De Sa Pereira, and Andrew P. Monkman

ACS Appl. Mater. Interfaces, **Just Accepted Manuscript** • DOI: 10.1021/acsami.8b15942 • Publication Date (Web): 01 Nov 2018Downloaded from <http://pubs.acs.org> on November 6, 2018**Just Accepted**

“Just Accepted” manuscripts have been peer-reviewed and accepted for publication. They are posted online prior to technical editing, formatting for publication and author proofing. The American Chemical Society provides “Just Accepted” as a service to the research community to expedite the dissemination of scientific material as soon as possible after acceptance. “Just Accepted” manuscripts appear in full in PDF format accompanied by an HTML abstract. “Just Accepted” manuscripts have been fully peer reviewed, but should not be considered the official version of record. They are citable by the Digital Object Identifier (DOI®). “Just Accepted” is an optional service offered to authors. Therefore, the “Just Accepted” Web site may not include all articles that will be published in the journal. After a manuscript is technically edited and formatted, it will be removed from the “Just Accepted” Web site and published as an ASAP article. Note that technical editing may introduce minor changes to the manuscript text and/or graphics which could affect content, and all legal disclaimers and ethical guidelines that apply to the journal pertain. ACS cannot be held responsible for errors or consequences arising from the use of information contained in these “Just Accepted” manuscripts.



Interfacial TADF Exciplex as a Tool to Localise Excitons, Improve Efficiency and Increase OLED Lifetime

Marco Colella^{†}, Piotr Pander[†], Daniel de Sa Pereira[†] and Andrew P. Monkman[†]*

[†] Physics Department, Durham University, South Road, Durham DH1 3LE, United Kingdom.

ABSTRACT

In this work, we employ a TADF exciplex formed between the emissive layer (EML) host, 26DCzPPy, and the electron transport layer (ETL), PO-T2T at the interface between the EML and the ETL to improve the stability and efficiency of a phosphorescence OLED based on Ir(dmpq)₂acac. We show that the presence of the TADF exciplex at the EML-ETL interface induces an efficient localisation of the recombination zone which is confined within the 5 nm thick EML. Furthermore, the TADF exciplex allows harvesting of the holes and electrons that piled-up at the EML-ETL interface and transfer the resultant excited state energy to the phosphorescent emitter through Förster and/or Dexter energy transfer. This approach

1
2
3 effectively improves the LT90 of devices from <1 min to 6 h by limiting recombination
4
5
6 processes outside of the 5 nm EML.
7
8
9

10
11 **KEYWORDS:** OLED, PhOLED, TADF, exciplex, photophysics, FRET, DET
12
13
14
15
16

17 INTRODUCTION

18
19 Since Tang and Van Slyke ¹ reported the first efficient multilayer organic light-emitting
20 diode (OLED), this field of research has grown extensively. Early research focused on
21 finding a solution to the problem of harvesting all the excitons produced by the electrical
22 excitation where now it focuses on maximising the fraction of emissive excited states
23 because spin statistics dictate that in the OLED, through electrical excitation, only 25%
24 of the excitons produced are singlets with the remaining 75% being triplets. In normal
25 fluorescent emitters, only singlets are allowed to decay radiatively leading to a huge loss of
26 internal efficiency of the OLED devices. A first solution to this problem was found using
27 organometallic complexes based on heavy metals like Iridium (Ir) and Platinum (Pt) ² to
28 produce phosphorescent OLEDs (PhOLEDs). In these compounds the singlets are
29 converted into triplets via intersystem crossing (ISC) which then can efficiently radiatively
30 decay due to the spin-orbit coupling induced from the presence of the heavy metal in the
31 compound. The second solution for harvesting all the electrically produced excited states
32 is via thermally-activated delayed fluorescence (TADF) ³. In this case, triplets can be up-
33 converted to singlets via reverse-ISC (rISC) and emit via normal fluorescence. The rISC
34 becomes efficient when the local excitonic triplet (³LE) and the charge transfer triplet state
35
36
37
38
39
40
41
42
43
44
45
46
47
48
49
50
51
52
53
54
55
56
57
58
59
60

1
2
3 (³CT), formed between a donor (D) and an acceptor (A) unit, are vibronically coupled ⁴
4
5
6 mediating the up-conversion rISC of the ³LE to the charge transfer singlet state (¹CT). The
7
8 same photophysical mechanism applies to both intra- and inter-molecular CT states ⁵. The
9
10 latter case is also called an exciplex state when the CT state is formed between two different
11
12 molecules. Efficiencies higher than 20% have been achieved with both approaches but
13
14 when considering a more practical application, research in OLEDs aims for efficiency but
15
16 also for small efficiency roll-off and long operational lifetime. Kondakova et al. in 2008
17
18 firstly reported on the performance enhancement of PhOLEDs when an exciplex co-host
19
20 is employed ⁶. Later, after Fukagawa et al. ⁷ demonstrated performance enhancement of
21
22 PhOLEDs when a TADF host was used, many other groups also published using either
23
24 TADF small molecules or exciplexes as hosts due to the effective Förster resonant energy
25
26 transfer (FRET) to the emitter that these systems can provide, jointly with the 100 % triplet
27
28 harvesting via the TADF mechanism ^{8–16}. Furthermore, Duan et al. ¹³ demonstrated that by
29
30 inserting a TADF exciplex at the interface between the host and the hole transport layer
31
32 (HTL) of a PhOLED, it is possible to enhance the stability and the performance of the device
33
34 exploiting the energy transfer from the interfacial exciplex and the guest material.
35
36
37
38
39
40
41
42
43
44

45 In this work, we investigated the effect of using such a strategy on the electron side of
46
47 the device to improve the charge balance of the devices. The electron mobility in the OLED
48
49 devices is indeed commonly lower than the hole mobility causing the holes to pile-up at
50
51 the interface between emissive layer (EML) and electron transport layer (ETL), which
52
53 could well be a source of device degradation. To address this problem, a TADF exciplex
54
55 formed by the well-known bipolar EML host 2,6-bis[3-(9H-carbazol-9-yl)phenyl]pyridine
56
57
58
59
60

1
2
3 (26DCzPPy) and the donor 2,4,6-tris[3-(diphenylphosphinyl)phenyl]-1,3,5-triazine (PO-
4
5
6 T2T) used as ETL, was introduced to avoid the pile-up problem. All the devices were doped
7
8 with bis(2-(3,5-dimethylphenyl)quinoline-C2,N')(acetylacetonato)iridium(III)
9
10 (Ir(dmpq)₂acac) to obtain efficient FRET from the interfacial exciplex due to the extensive
11
12 overlap of the absorption spectrum of the dopant with the exciplex emission as well as
13
14 yielding 100% phosphorescent emission. The molecular structure of the molecules
15
16 involved in the FRET process are shown in Figure 1a. Furthermore, we have employed a
17
18 device architecture with a 5 nm thick emissive layer (EML) that allowed us to assess the
19
20 localization of the recombination zone and obtain more information about the energy
21
22 transfer mechanisms between the exciplex and the dopant. We were indeed able to observe
23
24 when exciton localisation was lost simply by observing the changes in the
25
26 electroluminescence spectrum and relating those changes to the variations in the stability
27
28 of the device with the different device structures.
29
30
31
32
33
34
35

36
37 A maximum EQE of 28.6% at 100 cd/m² as well as a very low roll-off with an efficiency
38
39 of 25.2 % at 1000 cd/m² was achieved using this architecture. Further device structures
40
41 were used introducing a 1nm spacer layer between the EML and the exciplex, and by
42
43 substituting PO-T2T alternatively with 2,2',2''-(1,3,5-benzinetriyl)-tris(1-phenyl-1-H-
44
45 benzimidazole) (TPBi) and 2,9-dimethyl-4,7-diphenyl-1,10-phenanthroline (BCP) to
46
47 access the role of energy transfer to the Ir(dmpq)₂acac. All the results highlight the
48
49 importance of the energy transfer process from the interfacial exciplex to the
50
51 phosphorescent guest in the enhancement of both performances and stability of the
52
53 devices.
54
55
56
57
58
59
60

METHODS

The OLEDs from this study were fabricated on patterned ITO coated glass (Ossila) with a sheet resistance of 20 Ω /sq and ITO thickness of 100 nm. After loading the pre-cleaned substrates into a Kurt J. Lesker Spectros II deposition chamber, both the small molecules and the cathode layers were thermally evaporated with a pressure of no more than 10^{-6} mbar for a pixel size of 4.5 mm². The devices produced were then encapsulated using UV-curable epoxy (DELO Katiobond) alongside the edges of the active area with a glass coverslip (Ossila). The materials used for the production of the devices were, N,N'-di(1-naphthyl)-N,N'-diphenyl-(1,1'-biphenyl)-4,4'-diamine (NPB) and 4,4',4''-tris(carbazol-9-yl)triphenylamine (TCTA), used respectively as hole injection layer (HIL) and hole transporting layer (HTL). 2,4,6-tris[3-(diphenylphosphinyl)phenyl]-1,3,5-triazine (PO-T2T), 2,2',2''-(1,3,5-benzinetriyl)-tris(1-phenyl-1-H-benzimidazole) (TPBi) and 2,9-dimethyl-4,7-diphenyl-1,10-phenanthroline (BCP) as electron transporting layer (ETL) while lithium fluoride (LiF) and aluminium (Al) were used as an electron injection layer and cathode respectively. The 2,6-bis[3-(9H-carbazol-9-yl)phenyl]pyridine (26DCzPPy) was used as host material and bis(2-(3,5-dimethylphenyl)quinoline-C2,N')(acetylacetonato)iridium(III) (Ir(dmpq)₂acac) the emitting guest material. NPB, TCTA and BCP and TPBi were purchased from Sigma Aldrich and sublimed before being used in for the production of OLEDs. 26DCzPPy, Ir(dmpq)₂acac and PO-T2T were purchased respectively from Ossila and Lumtec and used as received. Steady-state absorption and emission spectra were acquired using a UV-3600 Shimadzu spectrophotometer and a Jobin Yvon Horiba Fluoromax-3 fluorometer, respectively. Time-

resolved spectra were obtained by exciting the sample with a Nd:YAG laser (EKSPLA), 10 Hz, 355 nm. Sample emission was detected with a gated iCCD camera (Stanford Computer Optics).

RESULTS AND DISCUSSION

26DCzPPy:PO-T2T photophysics

Although the 26DCzPPy:PO-T2T exciplex has been previously reported¹⁷ there has been little explanation to its photophysics. First of all, the exciplex photoluminescence (PL) decay at room temperature (figure 1c) is biexponential with prompt fluorescence (PF) decay time ($\tau_{PF} = 14.4 \pm 0.4$ ns) and delayed fluorescence (DF) decay time ($\tau_{DF} = 3.0 \pm 0.2$ μ s). From the integral of the PF and DF regions of the PL decay, figure S1, the ratio between the DF and PF contribution to the emission has been calculated (DF/PF \approx 2.5) while the rISC rate is 1.1×10^6 s⁻¹ calculated accordingly to the procedure published by Dias et al.¹⁸. The singlet-triplet gap is estimated to be $\Delta E_{ST} = 0.09$ eV. The delayed fluorescence changes its intensity with temperature as observed from exciplex photoluminescence decay between 295 and 80 K, Figure 1c, which indicates thermally-activated character. Furthermore, the delayed fluorescence component shows a laser fluence dependency with 0.92 exponent (figure 1d). This being close to 1, thus a linear relation, along with the strongly temperature dependent delayed fluorescence, Figure 1c, indicates TADF mechanism to be the main triplet harvesting mechanism involved (i.e. excluding triplet-triplet annihilation).

Interestingly, the prompt and delayed fluorescence spectra of the exciplex blend are clearly distinct, (figure S2). The early emission spectrum at 0.7 ns delay shows emission

1
2
3 maximum at ≈ 460 nm while at later time delays there is a gradual redshift observed and
4
5
6 the delayed fluorescence shows a maximum at ≈ 490 nm as for the steady state PL spectrum
7
8
9 showed in figure 1b. This behavior indicates a significant structural geometry re-
10
11 organization within the D and A molecules resulting in the charge transfer (CT) emissive
12
13 state energy relaxation. The TADF emission clearly dominates at 295 K, but at 80 K a weak
14
15 delayed fluorescence (1-100 μ s delay), is accompanied by phosphorescence emission (> 10
16
17 ms delay) of 26DCzPPy (see figure S2) ¹⁹. This observation suggests that the local triplet
18
19 state (³LE) of 26DCzPPy is coupled with the exciplex charge transfer (CT) state and the
20
21 coupling of ¹CT and ³CT with the ³LE gives rise to TADF in this system. In Figure 1b is
22
23 shown the extensive overlap between the absorption of Ir(dmpq)₂acac and the
24
25 26DCzPPy:PO-T2T PL which are necessary to provide efficient FRET between the exciplex
26
27 and the phosphorescent emitter.
28
29
30
31
32
33
34
35
36
37
38
39
40
41
42
43
44
45
46
47
48
49
50
51
52
53
54
55
56
57
58
59
60

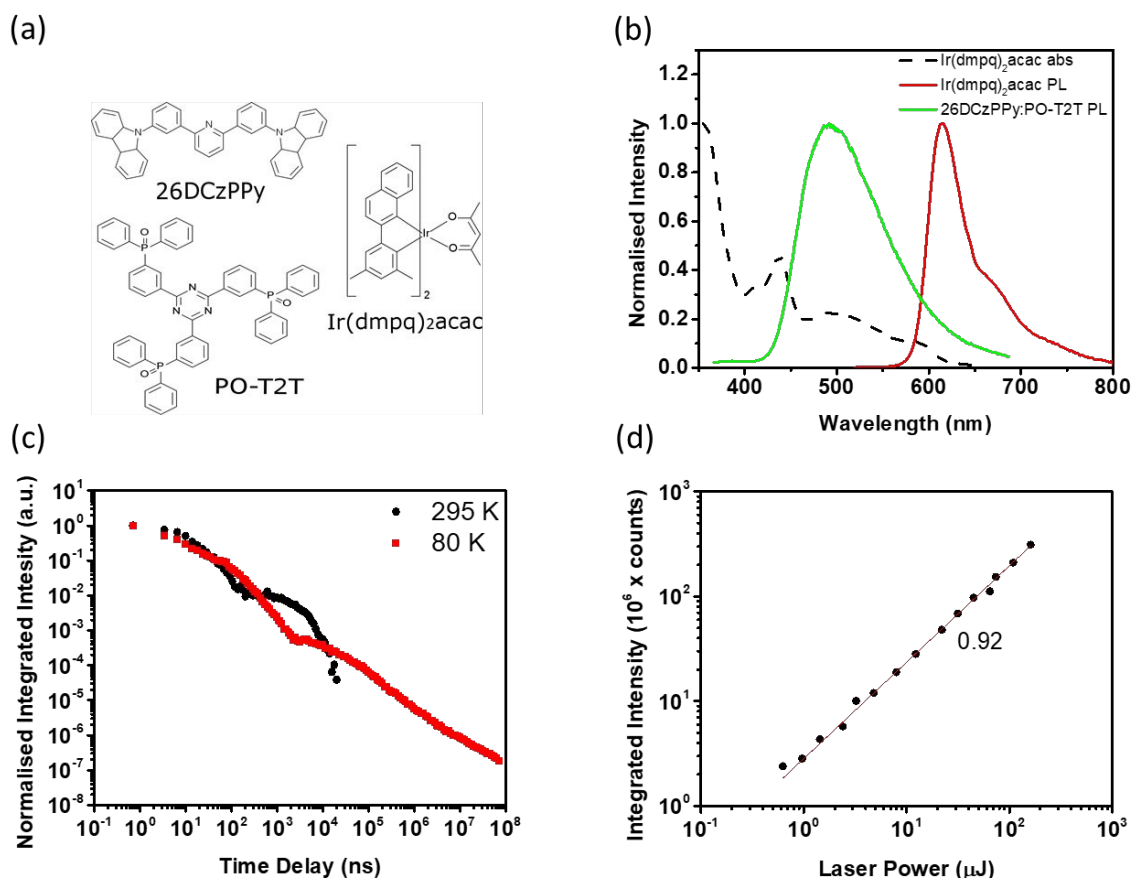


Figure 1 (a) Molecular structure of the exciplex forming donor (26DCzPPy), acceptor (PO-T2T) and phosphorescent emitter (Ir(dmpq)₂acac) used in this study. (b) The normalised absorption and PL spectra of Ir(dmpq)₂acac and 26DCzPPy:PO-T2T exciplex. (c) Time resolved fluorescence decay curves at 80 K and 295 K. (d) Integrated area as a function of the laser excitation (355 nm) of 26DCzPPy:PO-T2T exciplex blend.

PhOLEDs

Initially, we optimised the concentration of the dopant by implementing a device structure of NPB (40nm)|TCTA (10 nm)|26DCzPPy (5 nm)|1-4-10 wt% of Ir(dmpq)₂acac in 26DCzPPy (5 nm)|PO-T2T (50 nm)|LiF (1nm)|Al (100 nm) which are respectively labelled as Dev1, Dev2 and Dev3. The 5 nm buffer layer of 26DCzPPy was used to avoid direct

1
2
3 injection of holes from the TCTA layer into Ir(dmpq)₂acac to maximise the charge
4
5 recombination at the exciplex interface and therefore to help the energy transfer process
6
7 from the interfacial exciplex to the guest phosphor to dominate the device physics. The
8
9 slight redshift observed with the increased doping concentration in Figure 2c it is due to
10
11 reabsorption of the emitter emission. In fact, the emission and the absorption spectrum
12
13 overlap in the region between 550 and 650 nm showing a rather small Stokes shift as visible
14
15 in Figure 1b. In Figure 2a it can be seen that the current density of the devices increases
16
17 with the concentration of Ir(dmpq)₂acac in the EML. This is a typical behaviour in
18
19 PhOLEDs due to charge trapping on the Iridium complexes since they act as deep traps for
20
21 both holes and electrons²⁰. The energy difference between the HOMO and LUMO levels
22
23 of 26DCzPPy and Ir(dmpq)₂acac is 0.61 eV and 0.74 eV respectively^{10,21,22}. In terms of
24
25 efficiency, we find the device loaded with 4 wt% Ir(dmpq)₂acac, Dev2, to exhibit the
26
27 highest EQE at both reference brightness of 100 cd/m² and 1000 cd/m² of 28.6 % and 25.2
28
29 % respectively. We attribute this small roll-off to triplet-polaron quenching²³. In general,
30
31 all three devices show an efficiency roll-off of only 10 % between 100 cd/m² and 1000
32
33 cd/m². Interestingly the device with 1 wt% Ir(dmpq)₂acac, Dev1, shows similar
34
35 performances to the device with 10 wt% Ir(dmpq)₂acac, Dev3, up to the brightness of 2000
36
37 cd/m². Afterwards the efficiency drops significantly faster compared to the more heavily
38
39 doped devices. This can be explained comparing the electroluminescence (EL) spectra
40
41 shown in Figure 2c and 2d. The figures show the EL spectra at the same brightness of 1,000
42
43 cd/m² and 10,000 cd/m² respectively. No exciplex emission is visible in any of the devices
44
45 at 1,000 cd/m². However, in the spectra collected at brightness of 10,000 cd/m², Figure 2d,
46
47
48
49
50
51
52
53
54
55
56
57
58
59
60

Dev1 shows a strong exciplex emission at 471 nm, inset of Figure 2d, while this was not visible in either Dev2 or Dev3. This observation confirms that the exciplex is indeed populated and that, even at with a doping concentration as low as 1%, it can be fully harvested via FRET at moderately low current density. We therefore interpret the abrupt EQE roll off of Dev1 at high current density to be the consequence of reaching the saturation of the energy transfer process which leads to the exciplex peak to arise in the EL spectrum. The exciplex emission observed in the EL spectrum is blue shifted by ≈ 20 nm from the PL spectrum of Figure 1b due to the interfacial geometry of the exciplex under the influence of the electric field in the OLED structure.²⁴ It should also be considered that the EML thickness is only 5 nm which is within the typical triplet exciton diffusion length, making Dexter energy transfer (DET) from the 26DCzPPy-PO-T2T interface a non-negligible effect in this particular device structure especially with the increment of doping concentration²⁵.

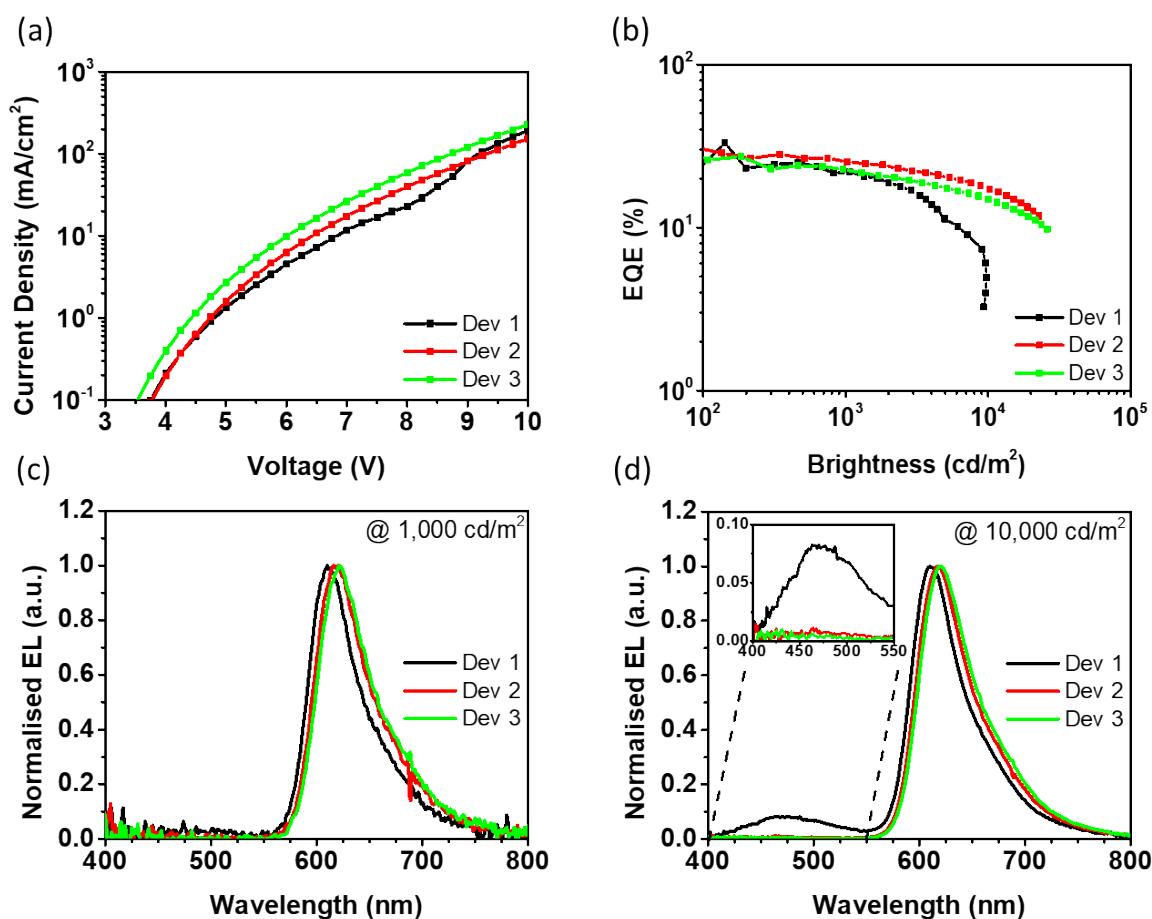
Table 1 Summary of the PhOLEDs performances at different doping level

wt%	@ 100 cd/m ²			@ 1000 cd/m ²			LT90 (h)
	V	cd/A	EQE	V	cd/A	EQE	
Ir(dmpq) ₂ acac							
Dev1 - 1 wt%	4.3	29.8 ± 9.1	24.5 ± 1.2	5.8	31.5 ± 0.9	21.9 ± 1.1	0.02
Dev2 - 4 wt%	4.3	36.6 ± 6.6	28.6 ± 1.4	5.5	30.7 ± 0.8	25.2 ± 1.3	1
Dev3 - 10 wt%	4.0	27.3 ± 4.5	26.0 ± 1.3	5.3	24.6 ± 0.5	22.7 ± 1.1	6
Dev4 - 4 wt% 1 nm spacer	4.3	26.0 ± 2.7	18.4 ± 0.9	5.3	23.4 ± 0.4	18.6 ± 0.9	1
Dev5 - 4 wt% TPBi	4.3	26.1 ± 3.9	15.6 ± 0.8	5.0	26.4 ± 0.5	21.3 ± 1.1	0.13

Dev6 - 7 wt% BCP	5.5	21.4 ± 2.9	31.5 ± 1.6	7.0	15.3 ± 0.4	15.3 ± 0.8	> 0.01
-----------------------------	-----	------------	------------	-----	------------	------------	--------

To separate the contributions of DET and FRET to the energy transfer process we produced devices with a 1 nm spacer layer introduced between the EML and the PO-T2T. The device structure used is NPB (40nm)|TCTA (10 nm)|26DCzPPy (5 nm)|4 wt% of Ir(dmpq)₂acac in 26DCzPPy (5 nm)|26DCzPPy (1 nm)|PO-T2T (50 nm)|LiF (1nm)|Al (100 nm) labelled Dev4. In Figure 4b we see that the performance of Dev4 is compared to Dev2 since both possess the same structure, differentiated only by the 1 nm spacer present in Dev4. At 100 cd/m² the EQE drops from 28.6 % measured for Dev2 to 18.4 % of Dev4 with the spacer, as summarised in Table 1, Dev4 maintains a constant EQE up to 1000 cd/m² with a value of 18.6 % showing that the device still possesses a good charge balance with the turn-on voltage unaffected by the 1 nm 26DCzPPy layer. In Figure 4c it is shown that at 1000 cd/m², no exciplex emission is visible in the EL spectrum, indicating that, all the exciplexes produced at the 26DCzPPy:PO-T2T interface are transferred via FRET to the dopant, since the DET has been greatly reduced by the spacer layer separation. On the other hand, in Figure 4d at a brightness of 10,000 cd/m² the exciplex emission is again clearly visible, at the same spectral position as observed for Dev1. The exciplex emission peaks at 471 nm indicating the incomplete energy transfer from the interfacial exciplex to the dopant. On the assumption that the 1 nm spacer layer does not affect the FRET efficacy and that DET must have been substantially eliminated²⁶. We attribute the difference in efficiency between the devices with and without the spacer to the effective suppression of the DET contribution. Thus, the exciplex emission appears at high brightness even at 4

1
2
3 wt% doped EML. This indicates that the process of energy transfer from the interfacial
4
5
6 exciplex to the dopant must be maximised to optimise the device efficiency.
7
8
9



41 **Figure 2** (a) JV and (b) EQE curves of the PhOLEDs with different doping level of
42 Ir(dmpq)2acac. Normalised EL spectra of the PhOLEDs at constant brightness of (c) 1000
43 cd/m² and (d) 10000 cd/m².
44
45
46
47
48
49

50
51 PO-T2T was then replaced with two standard electron transport materials, TPBi and
52 BCP. TPBi was chosen due to the very good LUMO alignment with 26DCzPPy, with a
53 $\Delta E_{\text{LUMO}} = 0.14 \text{ eV}$ ^{27,28}. BCP, on the other hand, was chosen because it has the very similar
54 LUMO energy to PO-T2T^{29,30}. Despite having the same LUMO level as PO-T2T, BCP does
55
56
57
58
59
60

not produce exciplex emission when blended with 26DCzPPy and neither does TPBi, figure S3 and S4.

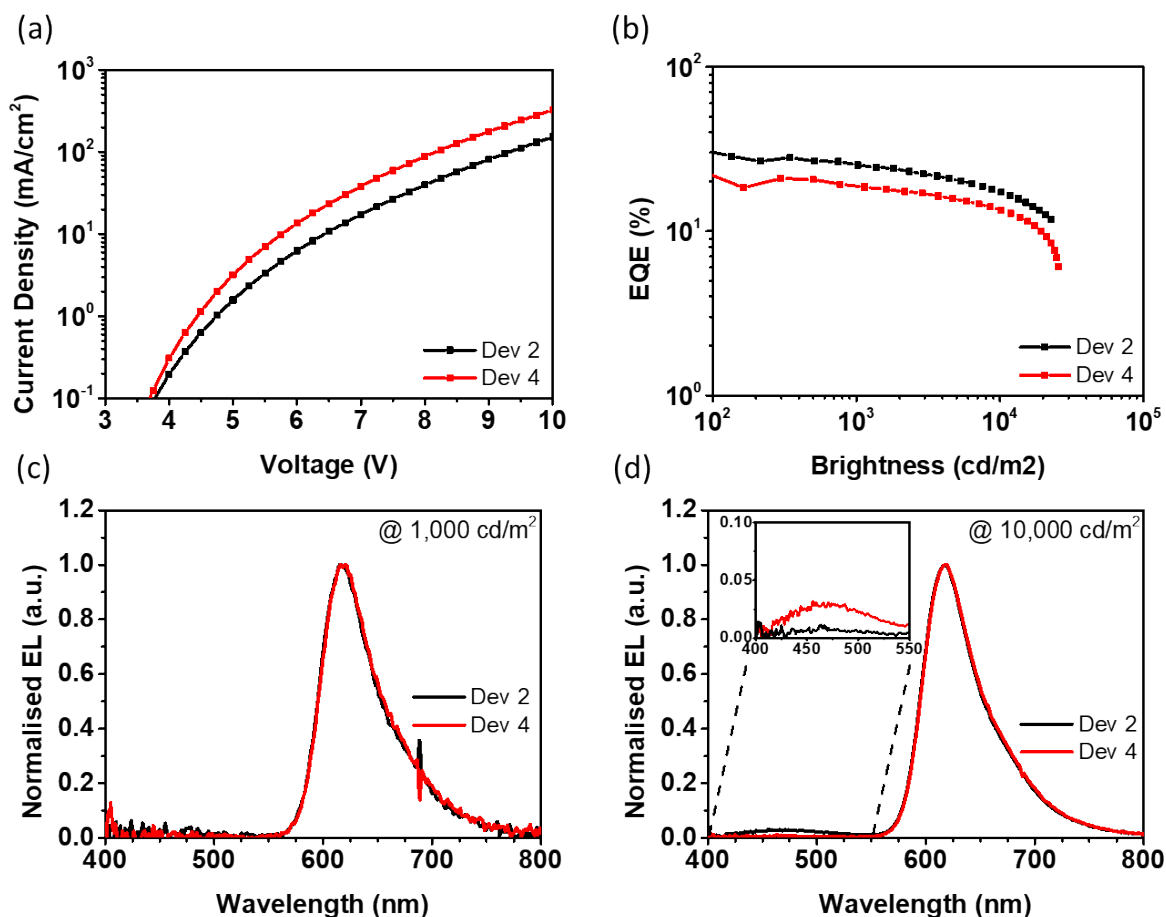


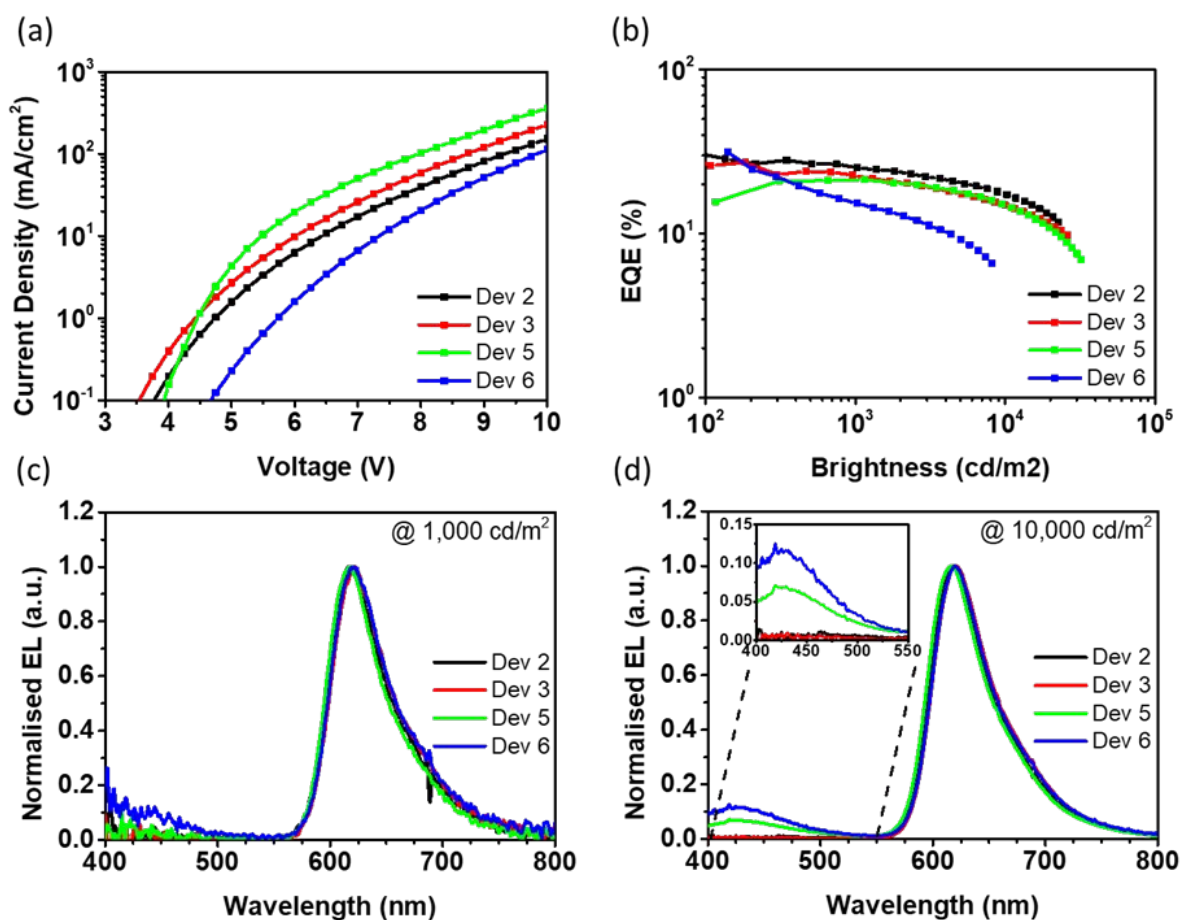
Figure 3 (a) JV and (b) EQE curves of the PhOLEDs with and without the 1 nm 26DCzPPy spacer layer at the EML|ETL interface. EL spectra of the PhOLEDs at constant brightness of (c) 1000 cd/m² and (d) 10000 cd/m².

In Figure 4 are shown the results for the PhOLEDs with the structures; NPB (40nm)|TCTA (10 nm)|26DCzPPy (5 nm)|4 wt% of Ir(dmpq)₂acac in 26DCzPPy (5 nm)|TPBi (50 nm)|LiF (1nm)|Al (100 nm) and NPB (40nm)|TCTA (10 nm)|26DCzPPy (5 nm)|7 wt% of Ir(dmpq)₂acac in 26DCzPPy (5 nm)|BCP (50 nm)|LiF (1nm)|Al (100 nm)

1
2
3 respectively labelled as Dev5 and Dev6. Dev5 shows lower performance with respect to the
4
5
6 exciplex enhanced devices, with good roll off and EQE of 21.3 % at 1000 cd/m², table 1.
7
8
9 The most interesting aspect is the substantial difference between the EQE obtained for the
10
11 same doping level of 4 wt%, at 100 cd/m². The device where TPBi (Dev5) is used shows a
12
13 build-in of efficiency with the EQE at 100 cd/m² of only 15.6 % compared to 28.6 % for
14
15 Dev2. The good resistance to roll-off is provided by the good energy level alignment with
16
17 the bipolar host 26DCzPPy that guarantees the balance of the charges in the EML. On the
18
19 other hand, the resulting performance is lower due to the absence of the energy transfer as
20
21 well as a recombination zone localization effect arising from the TADF exciplex. Evidence
22
23 of this is provided by comparing the EL spectra of the devices in Figure 4c and 4d. At 1,000
24
25 cd/m² only the emission from the Ir(dmpq)₂acac is observable whereas at 10,000 cd/m²
26
27 emission from the adjacent layer of 26DCzPPy is clearly visible, demonstrating the
28
29 broadening of the recombination zone with the increasing voltage in the absence of the
30
31 TADF exciplex at the host-ETL interface.
32
33
34
35
36
37
38
39

40 The same mechanism occurs when BCP is used to replace PO-T2T. In this last case, due
41
42 to the large electron injection barrier alongside the low conductivity of BCP itself ³¹, the
43
44 operational voltage increases substantially, as visible in Figure 4a, it increases from 4.3 V
45
46 with the exciplex to 5.5 V at 100 cd/m². The difference becomes even bigger at brightness
47
48 of 1000 cd/m² passing from 5.5 V with the exciplex to 7 V with the BCP layer. On the other
49
50 hand, when BCP is used, very high efficiency is found at 100 cd/m², 31.5 % out performing
51
52 all the other devices assessed in this work, Figure 4b. We consider this to be the effect of
53
54 the device structure used. We believe that at low voltage the electrons pile up at the ETL-
55
56
57
58
59
60

1
2
3 EML interface as they cannot easily overcome the injection barrier between the BCP and
4
5 26DCzPPy (0.34 eV) and are more likely to be directly injected into the Ir(dmpq)₂acac.
6
7
8 Once injected into the dopant the electrons are well confined by the 5 nm 26DCzPPy
9
10 undoped layer. The only possibility for the recombination is with the holes trapped by the
11
12 dopant giving rise at a very sharp emission onset at very low current and thus resulting in
13
14 extremely high efficiency thanks to the high PLQY of the Ir(dmpq)₂acac³². At higher
15
16 voltage the electrons possess enough potential energy to inject into the EML host, bypassing
17
18 this initially very efficient mechanism and causing the efficacy to reduce, halving the EQE
19
20 already at 1000 cd/m².
21
22
23
24
25
26
27
28
29
30
31
32
33
34
35
36
37
38
39
40
41
42
43
44
45
46
47
48
49
50
51
52
53
54
55
56
57
58
59
60



1
2
3 **Figure 4** (a) JV and (b) EQE curves of the PhOLEDs with BCP and TPBi as ETL and a 1 nm
4 spacer between the EML and PO-T2T. Normalised EL spectra of the PhOLEDs at constant
5 brightness of (c) 1000 cd/m² and (d) 10000 cd/m².
6
7
8
9

10
11
12
13
14 Among the devices produced in this study, the only one showing a detectable secondary
15 emission in the EL spectrum at 1000 cd/m², Figure 4c, is the device with BCP as ETL (Dev6),
16 confirming the earlier suggestion that, for this device, the electrons have enough potential
17 energy to overcome the injection barrier into the host which moves the recombination
18 zone towards the undoped 26DCzPPy layer. This effect is seen to increase at 10,000 cd/m²
19 where both TPBi and BCP show emission from the host at \approx 425 nm. The host emission in
20 the EL spectrum is redshifted of 33 nm from the PL (figure S3) again due to partial
21 reabsorption by the Ir complex. The secondary emission from the host is a clear sign of the
22 lost confinement of charge recombination in the EML.
23
24
25
26
27
28
29
30
31
32
33
34
35
36

37
38 Finally, in Figure 5 we compare the stability of the devices, obtained operating the
39 OLEDs at constant current with an initial brightness of 1000 cd/m². When the exciplex
40 interface is present in the device structure, the lifetime increases monotonically with the
41 concentration of dopant. We go from an LT90 of < 1 min at 1 wt% to \approx 1 hour at 4 wt%
42 and \approx 6 hours for 10 wt%. We attribute this increment to the increase of efficacy of the
43 energy transfer process due to the presence of a greater number of dopant molecules, thus
44 avoiding charge build up and quenching at the interface and degradation of the exciplex
45 itself. Interestingly, the behaviour of the device with the 1nm spacer layer (Dev 4) shows
46 the same LT90 as the one without the spacer layer (Dev 2) but then its decay rate
47
48
49
50
51
52
53
54
55
56
57
58
59
60

accelerates, with LT50 of 13.5 h with the 1nm spacer layer whereas the device without the spacers has an LT50 of 24 h. This difference in our opinion highlights the role of DET in reducing charge pile-up and thus degradation at the interface rapidly quenches DET. Moreover, PhOLEDs where BCP (Dev 6) and TPBi (Dev 5) were used showed LT90 of < 1 min and 8 minutes respectively. We attribute the longer LT90 obtained by the TPBi device over the BCP one to the better confinement of the recombination zone as showed from the EL spectra of Figure 4 and discussed above. This difference shows the importance of the presence of the interfacial exciplex. The exciplex reduces the charge pile up at the interface, and the degradation mechanism associated with it. The interfacial exciplex turns the piled-up charges into useful light that it is transferred to the Ir(dmpq)₂acac through FRET and DET. BCP device exhibits lower stability than TPBi due to the lost exciton confinement in the 5 nm thick EML spreading the recombination zone in non-efficient areas of the device, i.e. the undoped host.

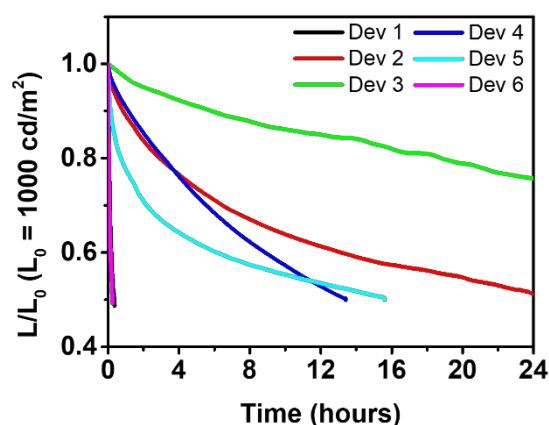


Figure 5 Luminescence decay of the OLEDs measured at constant current. All the devices kept at the current value that corresponds to the initial luminance of $L_0 = 1000 \text{ cd/m}^2$.

CONCLUSION

We successfully demonstrated that utilising a TADF exciplex at the interface between EML and ETL can improve the efficiency and stability of OLEDs. We highlight this improvement as a consequence of an extremely effective localisation of the excitons into the 5 nm EML. The interfacial exciplex not only localises the recombination zone onto the EML-ETL interface, it also harvests the holes and electrons piled-up at that interface forming exciplexes and recycling them into useful light in the emitter. We show clearly that both DET and FRET mechanisms are responsible for the energy transfer process from the exciplex to the dopant and that the DET process provides a very important contribution to the overall efficiency of the devices. Using the TADF exciplex interface layer on the electron side of the device greatly increases device lifetime LT90 from minutes to hours at 1000 cd/m². In the future, this strategy can be promising to be implemented in hyper fluorescent OLEDs to further improve the energy transfer mechanisms and boost the efficiency.

AUTHOR INFORMATION

Corresponding Author

Marco Colella, e-mail: marco.colella@durham.ac.uk

Notes

The authors declare no competing financial interests.

ACKNOWLEDGEMENTS

The authors would like to acknowledge the EXCILIGHT project funded by the European Union's Horizon 2020 Research and Innovation Programme under grant agreement No 674990.

ASSOCIATED CONTENT

Supporting Information.

Supplementary figures and discussions. This material is available free of charge via the Internet at <http://pubs.acs.org>

Photoluminescence decay with bi-exponential fit at 295 K. 295 K and 80K time resolved photoluminescence spectra of 26DCzPPy:PO-T2T exciplex. Photoluminescence spectra of 26DCzPPy, TPBi and 26DCzPPy:TPBi blend. Photoluminescence spectra of 26DCzPPy, BCP and 26DCzPPy:BCP blend.

1
2
3 **REFERENCES**
4
5
6
7

- (1) Tang, C. W.; VanSlyke, S. A. Organic Electroluminescent Diodes. *Appl. Phys. Lett.* **1987**, *51* (12), 913.
- (2) Baldo, M. A.; O'Brien, D. F.; You, Y.; Shoustikov, A.; Sibley, S.; Thompson, M. E.; Forrest, S. R. Highly Efficient Phosphorescent Emission from Organic Electroluminescent Devices. *Nature* **1998**, *395*, 151–154.
- (3) Uoyama, H.; Goushi, K.; Shizu, K.; Nomura, H.; Adachi, C. Highly Efficient Organic Light-Emitting Diodes from Delayed Fluorescence. *Nature* **2012**, *492* (7428), 234–238.
- (4) Dias, F. B.; Penfold, T. J.; Monkman, A. P. Photophysics of Thermally Activated Delayed Fluorescence Molecules. *Methods Appl. Fluoresc.* **2017**, *5*, 012001.
- (5) Dos Santos, P. L.; Dias, F. B.; Monkman, A. P. Investigation of the Mechanisms Giving Rise to TADF in Exciplex States. *J. Phys. Chem. C* **2016**, *120* (32), 18259–18267.
- (6) Kondakova, M. E.; Pawlik, T. D.; Young, R. H.; Giesen, D. J.; Kondakov, D. Y.; Brown, C. T.; Deaton, J. C.; Lenhard, J. R.; Klubek, K. P. High-Efficiency, Low-Voltage Phosphorescent Organic Light-Emitting Diode Devices with Mixed Host. *J. Appl. Phys.* **2008**, *104*, 094501.
- (7) Fukagawa, H.; Shimizu, T.; Kamada, T.; Kiribayashi, Y.; Osada, Y.; Hasegawa, M.; Morii, K.; Yamamoto, T. Highly Efficient and Stable Phosphorescent Organic Light-Emitting Diodes Utilizing Reverse Intersystem Crossing of the Host Material.

- 1
2
3 *Adv. Opt. Mater.* **2014**, *2*, 1070–1075.
- 4
5
6 (8) Fukagawa, H.; Shimizu, T.; Kamada, T.; Yui, S.; Hasegawa, M.; Morii, K.;
7
8 Yamamoto, T. Highly Efficient and Stable Organic Light-Emitting Diodes with a
9
10 Greatly Reduced Amount of Phosphorescent Emitter. *Sci. Rep.* **2015**, *5*, 9855.
- 11
12
13 (9) Fukagawa, H.; Shimizu, T.; Iwasaki, Y.; Yamamoto, T. Operational Lifetimes of
14
15 Organic Light-Emitting Diodes Dominated by Förster Resonance Energy Transfer.
16
17 *Sci. Rep.* **2017**, *7*(1), 1–8.
- 18
19
20 (10) Park, Y.-S.; Lee, S.; Kim, K.-H.; Kim, S.-Y.; Lee, J.-H.; Kim, J.-J. Exciplex-Forming
21
22 Co-Host for Organic Light-Emitting Diodes with Ultimate Efficiency. *Adv. Funct.*
23
24 *Mater.* **2013**, *23*(39), 4914–4920.
- 25
26
27 (11) Lee, S.; Koo, H.; Kwon, O.; Jae Park, Y.; Choi, H.; Lee, K.; Ahn, B.; Min Park, Y.
28
29 The Role of Charge Balance and Excited State Levels on Device Performance of
30
31 Exciplex-Based Phosphorescent Organic Light Emitting Diodes. *Sci. Rep.* **2017**, *7*
32
33 (1), 1–9.
- 34
35
36 (12) Duan, L.; Hou, L.; Lee, T.-W.; Qiao, J.; Zhang, D.; Dong, G.; Wang, L.; Qiu, Y.
37
38 Solution Processable Small Molecules for Organic Light-Emitting Diodes. *J. Mater.*
39
40 *Chem.* **2010**, *20*(31), 6392–6407.
- 41
42
43 (13) Zhang, D.; Cai, M.; Zhang, Y.; Bin, Z.; Zhang, D.; Duan, L. Simultaneous
44
45 Enhancement of Efficiency and Stability of Phosphorescent OLEDs Based on
46
47 Efficient Förster Energy Transfer from Interface Exciplex. *ACS Appl. Mater.*
48
49 *Interfaces* **2016**, *8*(6), 3825–3832.
- 50
51
52 (14) Zhao, B.; Zhang, T.; Chu, B.; Li, W.; Su, Z.; Wu, H.; Yan, X.; Fangming, J.; Gao, Y.;
53
54
55
56
57
58
59
60

- 1
2
3 Chengyuan, L. Highly Efficient Red OLEDs Using DCJTb as the Dopant and
4
5
6 Delayed Fluorescent Exciplex as the Host. *Sci. Rep.* **2015**, *5*, 10697.
7
8
9 (15) Sarma, M.; Wong, K. T. Exciplex: An Intermolecular Charge-Transfer Approach for
10
11 TADF. *ACS Appl. Mater. Interfaces* **2018**, *10*(23), 19279–19304.
12
13
14 (16) Zhang, D.; Duan, L.; Zhang, D.; Qiu, Y. Towards Ideal Electrophosphorescent
15
16 Devices with Low Dopant Concentrations : The Key Role of Triplet up-Conversion.
17
18 *J. Mater. Chem. C* **2014**, *2*, 8983–8989.
19
20
21 (17) Liu, X.-K.; Chen, W.; Thachoth Chandran, H.; Qing, J.; Chen, Z.; Zhang, X.-H.;
22
23 Lee, C.-S. High-Performance, Simplified Fluorescence and Phosphorescence
24
25 Hybrid White Organic Light-Emitting Devices Allowing Complete Triplet
26
27 Harvesting. *ACS Appl. Mater. Interfaces* **2016**, *8*(39), 26135–26142.
28
29
30
31 (18) Dias, F. B.; Penfold, T. J.; Monkman, A. P. Photophysics of Thermally Activated
32
33 Delayed Fluorescence Molecules. *Methods Appl. Fluoresc.* **2017**, *5*(1), 012001.
34
35
36
37 (19) Su, S.-J.; Sasabe, H.; Takeda, T.; Kido, J. Pyridine-Containing Bipolar Host Materials
38
39 for Highly Efficient Blue Phosphorescent OLEDs. *Chem. Mater* **2008**, *20*(5), 1691–
40
41 1693.
42
43
44
45 (20) Gong, X.; Ostrowski, J. C.; Moses, D.; Bazan, G. C.; Heeger, A. J.
46
47 Electrophosphorescence from a Polymer Guest-Host System with an Iridium
48
49 Complex as Guest: Förster Energy Transfer and Charge Trapping. *Adv. Funct.*
50
51 *Mater.* **2003**, *13*(6), 439–444.
52
53
54
55 (21) Lin, W.; Huang, W.; Huang, M.; Fan, C.; Lin, H.-W.; Chen, L.-Y.; Liu, J.-S.; Chao,
56
57 T.-C.; Tseng, M.-R. A Bipolar Host Containing Carbazole/Dibenzothiophene for
58
59
60

- 1
2
3 Efficient Solution-Processed Blue and White Phosphorescent OLEDs. *J. Mater.*
4
5
6 *Chem. C* **2013**, *1*, 6835–6841.
7
- 8 (22) Soon, B.; Jeon, O.; Yook, K. S.; Joo, C. W.; Lee, J. Y. Phenylcarbazole-Based
9
10 Phosphine Oxide Host Materials For High Efficiency In Deep Blue Phosphorescent
11
12 Organic LightEmitting Diodes. *Adv. Funct. Mater.* **2009**, *19*, 3644–3649.
13
14
15
- 16 (23) Song, D.; Zhao, S.; Luo, Y.; Aziz, H. Causes of Efficiency Roll-off in Phosphorescent
17
18 Organic Light Emitting Devices : Triplet-Triplet Annihilation versus Triplet-
19
20 Polaron Quenching. *Appl. Phys. Lett.* **2010**, *97*, 243304.
21
22
23
- 24 (24) Al Attar, H. A.; Monkman, A. P. Electric Field Induce Blue Shift and Intensity
25
26 Enhancement in 2D Exciplex Organic Light Emitting Diodes; Controlling Electron-
27
28 Hole Separation. *Adv. Mater.* **2016**, *28*, 8014–8020.
29
30
31
- 32 (25) O'Brien, D. F.; Baldo, M. A.; Thompson, M. E.; Forrest, S. R. Improved Energy
33
34 Transfer in Electrophosphorescent Devices. *Appl. Phys. Lett.* **1999**, *74*, 442.
35
36
37
- 38 (26) Luhman, W. A.; Holmes, R. J. Investigation of Energy Transfer in Organic
39
40 Photovoltaic Cells and Impact on Exciton Diffusion Length Measurements. *Adv.*
41
42 *Funct. Mater.* **2011**, *21*, 764–771.
43
44
- 45 (27) Cai, C.; Su, S.; Chiba, T.; Sasabe, H.; Pu, Y.; Nakayama, K.; Kido, J. High-Efficiency
46
47 Red , Green and Blue Phosphorescent Homojunction Organic Light-Emitting
48
49 Diodes Based on Bipolar Host Materials. *Org. Electron.* **2011**, *12*, 843–850.
50
51
52
- 53 (28) Jankus, V.; Chiang, C. J.; Dias, F.; Monkman, A. P. Deep Blue Exciplex Organic
54
55 Light-Emitting Diodes with Enhanced Efficiency; P-Type or E-Type Triplet
56
57 Conversion to Singlet Excitons? *Adv. Mater.* **2013**, *25* (10), 1455–1459.
58
59
60

- 1
2
3
4
5
6
7
8
9
10
11
12
13
14
15
16
17
18
19
20
21
22
23
24
25
26
27
28
29
30
31
32
33
34
35
36
37
38
39
40
41
42
43
44
45
46
47
48
49
50
51
52
53
54
55
56
57
58
59
60
- (29) Adamovich, V.; Brooks, J.; Tamayo, A.; Alexander, A. M.; Djurovich, P. I.; Andrade, B. W. D.; Adachi, C.; Forrest, R.; Thompson, M. E. High Efficiency Single Dopant White Electrophosphorescent Light Emitting Diodes. *New J. Chem.* **2002**, *26*, 1171–1178.
- (30) Hung, W. Y.; Fang, G. C.; Lin, S. W.; Cheng, S. H.; Wong, K. T.; Kuo, T. Y.; Chou, P. T. The First Tandem, All-Exciplex-Based Woled. *Sci. Rep.* **2014**, *4*, 4–9.
- (31) Wu, I. W.; Wang, P. S.; Tseng, W. H.; Chang, J. H.; Wu, C. I. Correlations of Impedance-Voltage Characteristics and Carrier Mobility in Organic Light Emitting Diodes. *Org. Electron. physics, Mater. Appl.* **2012**, *13* (1), 13–17.
- (32) Kim, D. H.; Cho, N. S.; Oh, H. Y.; Yang, J. H.; Jeon, W. S.; Park, J. S.; Suh, M. C.; Kwon, J. H. Highly Efficient Red Phosphorescent Dopants in Organic Light-Emitting Devices. *Adv. Mater.* **2011**, *23* (24), 2721–2726.

TOC

